Astronomy & Astrophysics manuscript no. ms
October 15, 2009

The nature of the X-ray binary IGR J19294+1816 from *INTEGRAL*, *RXTE*, and *Swift* observations

J. Rodriguez[1], J.A. Tomsick[2], A. Bodaghee[2], J.-A. Zurita Heras[1], S. Chaty[1], A. Paizis[3], S. Corbel[1]

[1] Laboratoire AIM, CEA/DSM - CNRS - Université Paris Diderot (UMR 7158), CEA Saclay, DSM/IRFU/SAp, F-91191 Gif-sur-Yvette, France
[2] Space Science Laboratory, 7 Gauss Way, University of California, Berkeley, C1 94720-7450, USA
[3] INAF-IASF, Sezione di Milano, via Bassini 15, 20133 Milano, Italy

Preprint online version: October 15, 2009

ABSTRACT

We report the results of a high-energy multi-instrumental campaign with *INTEGRAL*, *RXTE*, and *Swift* of the recently discovered *INTEGRAL* source IGR J19294+1816. The *Swift*/XRT data allow us to refine the position of the source to $RA_{J2000}= 19^h\ 29^m\ 55.9^s$ $Dec_{J2000}=+18^\circ\ 18'\ 38.4''$ ($\pm3.5''$), which in turn permits us to identify a candidate infrared counterpart. The *Swift* and *RXTE* spectra are well fitted with absorbed power laws with hard ($\Gamma \sim 1$) photon indices. During the longest *Swift* observation, we obtained evidence of absorption in true excess to the Galactic value, which may indicate some intrinsic absorption in this source. We detected a strong (P=40%) pulsation at 12.43781($\pm$0.00003) s that we interpret as the spin period of a pulsar. All these results, coupled with the possible 117 day orbital period, point to IGR J19294+1816 being an HMXB with a Be companion star. However, while the long-term *INTEGRAL*/IBIS/ISGRI 18–40 keV light curve shows that the source spends most of its time in an undetectable state, we detect occurrences of short ($\sim 2000-3000$ s) and intense flares that are more typical of supergiant fast X-ray transients. We therefore cannot make firm conclusions on the type of system, and we discuss the possible implications of IGR J19294+1816 being an SFXT.

Key words. X-rays: binaries ; Accretion, accretion disks ; Stars: individual: IGR J19294+1816, IGR J11215−5952, IGR J18483−0311

1. Introduction

The INTErnational Gamma-Ray Astrophysics Laboratory (*INTEGRAL*) has permitted a large number of new sources to be discovered. Amongst the $\sim$ 250 new sources[1], *INTEGRAL* has unveiled two new or poorly-known types of high mass X-ray binaries (HMXB): the very absorbed supergiant HMXBs, and the supergiant fast X-ray transients (SFXT). While all types of HMXBs (including those hosting a Be star, Be-HMXBs) are powered by accretion of material by a compact object, understanding the nature of a system is very important for studying the evolutionary paths of source populations, and more globally, the evolution of the Galaxy in terms of its source content.

IGR J19294+1816 was discovered by Tuerler et al. (2009) who reported activity of this source seen with *INTEGRAL* during the monitoring campaign of GRS 1915+105 (e.g. Rodriguez et al., 2008a). Archival *Swift* data of a source named Swift J1929.8+1818 allowed us to give a refined X-ray position of $RA_{J2000}= 19^h\ 29^m\ 55.9^s$ and $Dec_{J2000}=+18^\circ\ 18'\ 39''$ ($\pm3.5''$) which we used to locate a possible infrared counterpart (Rodriguez et al., 2009). We also suggested that the *Swift* and *INTEGRAL* sources are the same and that activity from IGR J19294+1816 had been seen with *Swift* in the past. The temporal analysis of the XRT light curve showed a possible pulsation at 12.4 s (Rodriguez et al., 2009). Analysis of *Swift*/BAT archival data revealed that the source had been detected on previous occasions with a periodicity at 117.2 days (Corbet & Krimm, 2009) that we interpreted as the orbital period of the system.

Soon after the discovery of the source with *INTEGRAL*, we triggered our accepted *RXTE* and *Swift* programmes for follow-up observations of new *INTEGRAL* sources (PI Rodriguez). A preliminary analysis of the real-time *RXTE* data allowed us to confirm the pulsations in the signal from the source (Strohmayer et al., 2009) at a barycentred period of 12.44 s indicating that this object hosts an accreting X-ray pulsar. Here we report the detailed analysis of the *INTEGRAL*, *Swift*, and *RXTE* observations. We begin this paper by detailing the procedures employed for the data reduction. We then describe the results (refined position, X-ray spectral, and temporal analyses) in Sects. 3, 4, 5, and 6, and discuss them in Sect. 7.

2. Observations and data reduction

The log of the *Swift* and *RXTE* observations of IGR J19294+1816 is given in Table 1. The `LHEASOFT v6.6.2` suite was used to reduce the *Swift* and *RXTE* data. The *RXTE*/PCA data were reduced in a standard way, restricting it to the times when the elevation angle above the Earth was greater than 10°, and when the offset pointing was less than 0.02°. We accumulated spectra from the top layer of proportional counter unit 2 (PCU 2), the only one that was active during all the observations, and therefore time-filtered the data for PCU 2 breakdown. The background was estimated using the faint model. In addition, we produced event files from `Good Xenon` data with `make_se`, from which we extracted 2^{-12} s ($\sim 250\ \mu$s) light curves between 2 and 20.2 keV (absolute channels 5 to 48 in order to limit the instrumental background at low and high

Send offprint requests to: J. Rodriguez e-mail: `jrodriguez@cea.fr`

[1] see http://isdc.unige.ch/~rodrigue/html/igrsources.html for an up to date list of all sources and their properties.

Table 1. Journal of the *Swift* and *RXTE* dedicated observations. Obs. S3 and X5 were simultaneous with an *INTEGRAL* observation.

Satellite	Date start (MJD)	Exposure time (s)	Name
Swift	54443.051	7959	S1
Swift	54447.013	3457	S2
RXTE	54921.315	2600	X1
RXTE	54921.708	3344	X2
RXTE	54922.813	3344	X3
RXTE	54923.730	1440	X4
Swift	54925.814	2565	S3
RXTE	54925.826	3360	X5

energies) with `seextrct`. Light curves with 1-s time resolution were obtained in the 2–60 keV range from standard 1 data. These light curves were then corrected for the background and used for the temporal analysis.

The *Swift*/XRT data were first processed with the `xrtpipeline v0.12.2` tool to obtain standardly filtered level 2 event files. Images, light curves, and spectra were extracted within `XSELECT V2.4a`. Source light curves and spectra were extracted from a circular region of 20 pixels radius centred on the most accurate source position available. We tested different regions of extraction for the background light curves and spectra, and obtained no significant differences. For the remainder of the analysis, the background region is a circular region of 60 pixels radius centred at RA=19^h 29^m 41.8^s and Dec=+18° 21′ 11.5″. The ancillary response file was obtained with `xrtmkarf 0.5.6` after taking the exposure map into account (see Rodriguez et al., 2008b, for more details).

We also analysed *all INTEGRAL* public pointings aimed at less than 10° from the position of IGR J19294+1816 plus all private data of our monitoring campaign on GRS 1915+105. The `Offline Scientific Analysis Software (OSA) v7.0` was used for the *INTEGRAL* data reduction. We further filtered the list of science windows (SCW) to those where the good exposure time of ISGRI was greater than 1000 s. After omitting the bad pointings (e.g. first or last pointings before the instruments are switched off due to passage through the radiation belts) this resulted in a total of 1476 good SCWs. These pointings were blindly searched for the presence of the source (see Rodriguez et al. (2008a) for the procedure of data reduction and source searching). An updated catalogue containing IGR J19294+1816 with the most precise *Swift* position was given as an input to the software. Mosaics were accumulated on a revolution basis, but this results in mosaics of very different exposure times. Note that even in revolution 788, where we confirm the detection reported by Tuerler et al. (2009), the source is too dim for further spectral analysis.

3. IGR J19294+1816 as seen with *INTEGRAL*

IGR J19294+1816 was discovered on March 27, 2009 (revolution 788, MJD 54917 Tuerler et al., 2009). A re-analysis of the consolidated data allowed us to confirm a source detection during this observation. The source was detected at 10.7 σ between 18 and 40 keV, with a flux of about 17 mCrab[2]. A re-analysis of the previous observation on March 21, 2009 (rev. 786, MJD 54911), led to a detection in the 18–40 keV energy range with a significance of 4.5 σ and a flux of 7.2 mCrab. IGR J19294+1816 was not detected on April 4, 2009 (rev 790, MJD 54925) with a 18–40 keV 3-σ upper limit of about 5 mCrab. The source was not detected in any of the mosaics from the previous revolution. However, given the very different exposure times we used in building the mosaics and the periodicity of the source activity seen with *Swift*/BAT (Corbet & Krimm, 2009), this may simply indicate that the periods of activity of the source are short.

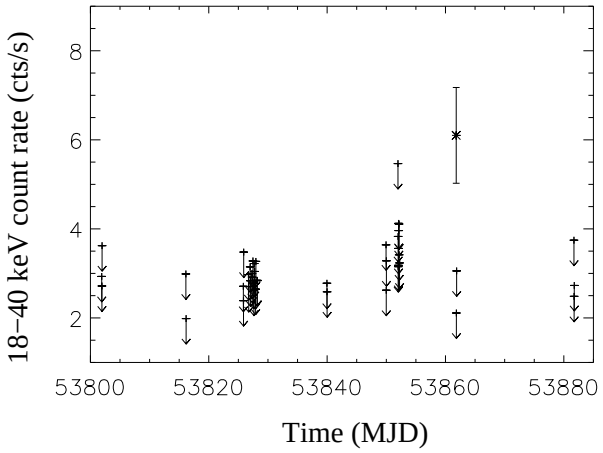

Fig. 1. *INTEGRAL*/IBIS 18–40 keV light curve of IGR J19294+1816 showing the flare on MJD 53861.

Examining these data on a SCW basis shows that the source was detected on a few occurrences. In particular, it was clearly detected during an observation in rev. 435 (MJD 53861) and during another pointing in rev. 482 (MJD 54004). In the former, IGR J19294+1816 was detected in SCW 9 (19.17–19.77 h UTC) with a 18–40 keV flux of 33.7 mCrab. It was not detected in the following SCW (19.85–20.50 h) with a 3-σ upper limit of 11.6 mCrab. No pointings are available before SCW 9. The 18–40 keV light curve of this epoch is reported in Fig. 1. In rev. 482, the source was detected in SCW 51 (1.05–2.03 h UTC) at a 18–40 keV flux of 22 mCrab (5.4 σ). It was not detected in the previous and following SCWs with respective 3-σ upper limits of 11.0 and 13.9 mCrab.

4. Refining the X-ray position, and the search for counterparts

We combined all *Swift* observations to create a mosaic image of the field. As shown in Fig. 2, a single bright X-ray source can be seen within the ∼ 5′ 90% error circle of the *INTEGRAL* position given in Tuerler et al. (2009). This source lies at (as obtained with `xrtcentroid`) RA_{J2000}=19^h 29^m 55.9^s and Dec_{J2000}=+18° 18′ 38.4″ with an uncertainty of 3.5″. Note that this is slightly different from the preliminary position given in Rodriguez et al. (2009), but the two positions are clearly compatible. Given the addition, here, of an additional *Swift* pointing to obtain these coordinates, we consider this position as the most precise one.

We searched for counterparts in catalogues available online such as the 2 Microns All Sky Survey point source and extended source catalogues[3] (2MASS and 2MASX, Skrutskie et al., 2006), the National Radio Astronomy Observatory VLA Sky

[2] The count rate to Crab conversion is based on an analysis of the Crab observation performed during rev. 774, with 1 $Crab_{18-40keV}$ = 181.1 cts/s.

[3] http://www.ipac.caltech.edu/2mass/

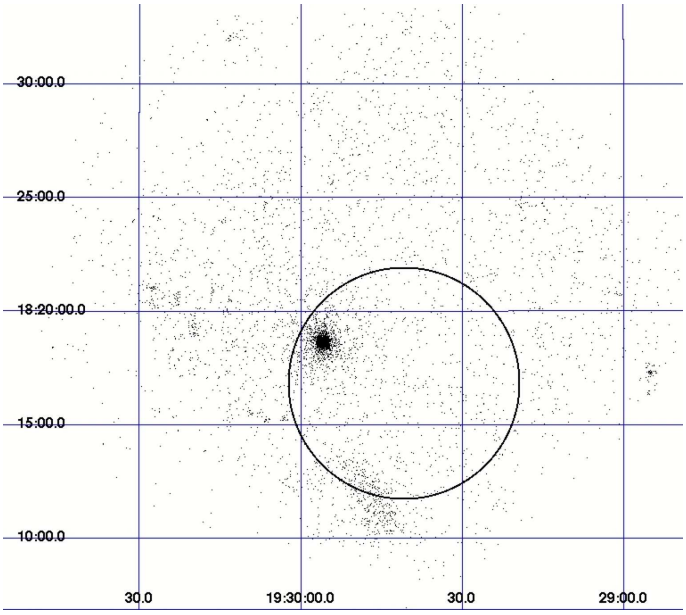

Fig. 2. *Swift*/XRT mosaic of the field around IGR J19294+1816. The circle represents the error box from *INTEGRAL*.

Table 2. Infrared magnitudes dereddened with different values of the absorption.

N_H $\times10^{22}$ cm^{-2}	A_V	$J_{der.}$	$H_{der.}$	$K_{s,der.}$	J-H	H-K_s
2.0	11.20	11.32	11.04	10.86	0.28	0.18
2.73	15.29	10.14	10.32	10.40	−0.18	−0.08
4.0	22.40	8.08	9.09	9.53	−1.01	−0.44

Survey (NVSS, Condon et al., 1998), and the catalogue of the US Naval Observatory (USNO[4]). We also made use of images from the Second Palomar Observatory Sky Survey obtained through the STScI Digitized Sky Survey (DSS[5]). Finding charts from 2MASS IR and DSS are shown in Fig. 3.

A single infrared counterpart is listed in the 2MASS catalogue: 2MASS J19295591+1818382 has magnitudes J=14.56 ±0.03, H=12.99 ±0.02, and K_s=12.11 ±0.02. No optical or radio counterpart was found in any of the other catalogues, although a faint object might be present in the "infrared" (7000–9700Å) POSS II image (Fig. 3). The infrared magnitudes were dereddened using $A_\lambda = C(\lambda)\times A_V$, with $C(\lambda)$ the wavelength dependent coefficients obtained by Cardelli et al. (1989) (see Table 4 in Rahoui et al., 2008, for the values adopted), and A_V=5.6×10^{22}× N_H (Predehl & Schmitt, 1995). The value of the total absorbing column density along the line of sight was obtained from the LAB survey of Galactic HI (Kalberla et al., 2005), and the CO survey of Dame et al. (2001) for the value of molecular H_2. Therefore, $N_H = N_{HI} + 2N_{H_2} = 1.23 + 2 \times 0.75 = 2.73\times10^{22}$ cm^{-2}. We also used the value of N_H obtained through the X-ray spectral fits to the data, $N_{HX,bbody}$=2.0×10^{22} cm^{-2}, and $N_{HX,po}$= 4.0×10^{22} cm^{-2} (see Sec. 5). The dereddened magnitudes are reported in Table 2.

[4] http://www.usno.navy.mil/USNO/astrometry/optical-IR-prod/icas
[5] http://archive.stsci.edu/cgi-bin/dss_form

5. X-ray spectral analysis

5.1. Correction of the Galactic ridge emission in the PCA spectra

Since IGR J19294+1816 is faint and located in the Galactic plane (its Galactic coordinates are l = 53.5400°, b = 0.1150°), the Galactic ridge can contribute a significant amount of the flux collected by the PCA. We estimated the level of emission using the results from Valinia & Marshall (1998), and first corrected the spectra from the Galactic ridge emission in a similar way as done for IGR J19140+0951 by Prat et al. (2008), i.e. adding the Galactic ridge spectrum to the instrumental background spectrum.

A simultaneous fit to the S3 and X5 spectra showed a large offset in the normalisations of the spectra: when including a constant in the fit and freezing it to 1 for the S3 spectrum it resulted in a low value of ∼0.45 for the X5 spectrum. This might indicate that either the source varied during the non-simultaneous part of these observations, or that we over-corrected the emission of the Galactic ridge in the PCA spectrum. We consider this last hypothesis as the most likely given that the spectrum of the Galactic ridge obtained from Valinia & Marshall (1998) is an average spectrum covering the central regions of the Galaxy, i.e. $-45° < l < 45°$ and $-1.5° < b < 1.5°$, and that IGR J19294+1816 is slightly outside this region. Although the source is located in the Galactic ridge, we can expect local variations in the ridge, and/or slight changes (lower intensity for example) at high longitude (as also mentioned in Valinia & Marshall, 1998).

In a second run, we did not correct the X5 spectrum for the contribution of the Galactic ridge, and we did not include a normalisation constant between the S3 and X5 spectra (we therefore made the assumption that *Swift* and *RXTE* are perfectly cross calibrated). The spectra were fit with an absorbed power law and the best-fitting model for the Galactic ridge spectrum obtained by Valinia & Marshall (1998). A multiplicative constant precedes this spectral component whose parameters are frozen. The spectral model is therefore `phabs*powerlaw+constant*(wabs*(raymond+powerlaw))` in the `XSPEC` terminology. We initially fitted the S3 spectrum alone (with the constant fixed at 0) to obtain the parameters of the source. Then, we added the X5 spectrum and only left the normalisation constant to the X5 data free to vary while it was held at 0 for the S3 data. Therefore, we assume that the average spectral parameters obtained in the $-45° < l < 45°$ are still valid at the position of IGR J19294+1816 , and that only the overall flux of the ridge emission changes. The most precise value obtained for the constant is 0.85±0.04 (at 90% confidence). In subsequent analyses, we used this value to correct all PCA spectra according to:

$$\mathrm{BGD_{tot}} = \mathrm{BGD_{instr}} + 0.85 \times \mathrm{Ridge} \quad (1)$$

5.2. Results of the spectral analysis

The *Swift*/XRT spectra were rebinned so as to have a minimum of 20 cts per channel, except for the channels below about 1.2 keV that were grouped in 2 bins: one below 0.2 keV that was not considered further for the spectral fitting, and one between 0.2–1.2 keV to obtain an additional spectral point to better constrain the absorption column density N_H. The *Swift* spectra were fitted between ∼ 0.8 and ∼ 8 keV, while the *RXTE* spectra were fitted between 3 and 25 keV. We fitted each individual spectrum alone in `XSPEC 11.3.2ag`, except the spectra from observations

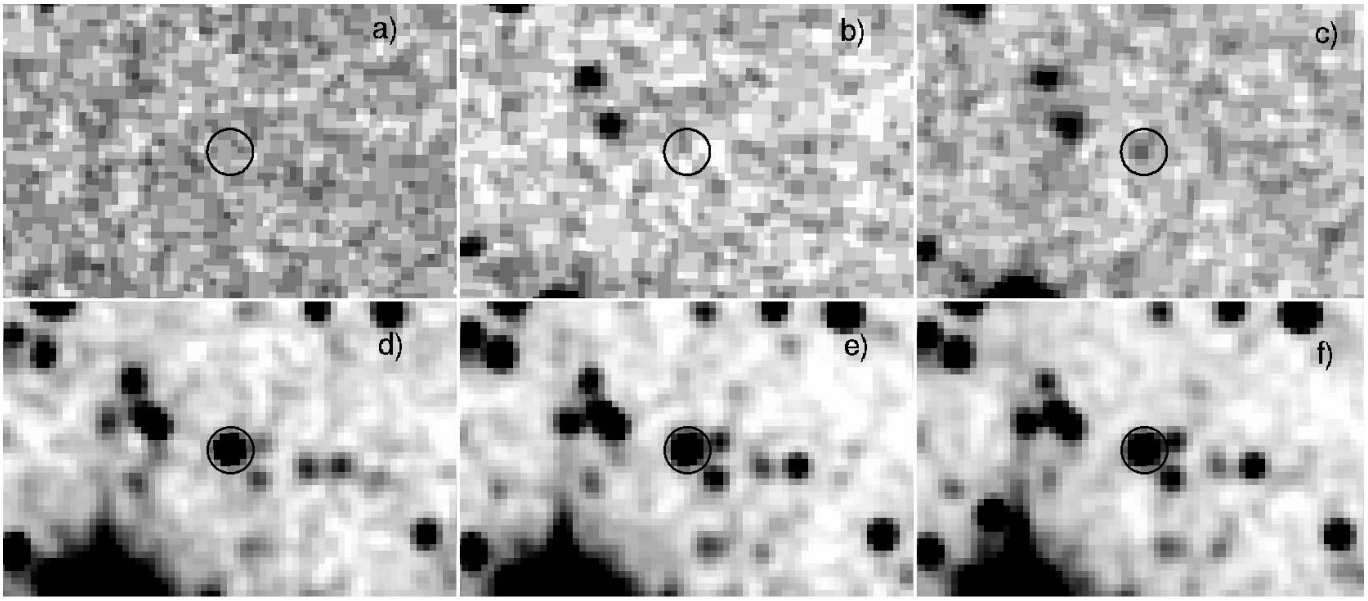

Fig. 3. 1.14′×0.73′ POSS II optical (top) and 2MASS infrared (bottom) images of the field around IGR J19294+1816. The black circle is the *Swift* error box. a) " Blue", b) "Red", c) "infrared", d) J filter e) H filter, f) K_s filter.

S3 and X5 that were fitted simultaneously. Different spectral models were used to fit the spectra. The *Swift* spectra are well fitted using either an absorbed blackbody or an absorbed power law. Only the latter model provides a good fit to the *RXTE* spectrum, and joint *Swift* and *RXTE* spectra. Considering the detection at energies greater than 20 keV with *INTEGRAL* and *Swift* , this suggests that the true origin of the emission is probably not from a blackbody. However, we report the parameters of the blackbody together with those obtained with the power-law model in Table 3. Observations S3 and X5 were simultaneous with an *INTEGRAL* observation, but the source was not detected by the latter satellite with an 18–40 keV 3-σ upper limit of 5 mCrab with IBIS.

Since the PCA is well calibrated only above 3 keV, it is not suitable for proper measures of N_H, especially in such a dim source. In fact, leaving all parameters free to vary during the spectral fits leads to poorly-constrained values for this parameter ($N_H < 5.4 \times 10^{22}$ cm^{-2} in Obs. X1). We therefore froze the value of N_H to the value returned by the fit to the closest *Swift* data (Obs. S3 which, simultaneously fitted with X5, leads to 3.4×10^{22} cm^{-2} for a power-law model).

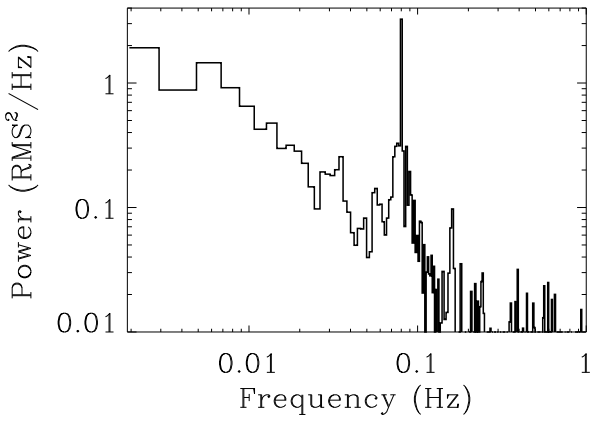

Fig. 4. 0.00195–1 Hz white-noise corrected power spectral density distribution of *RXTE* Obs. 1 & 3 obtained from the 2–20.2 keV high-resolution light curve.

6. X-ray temporal analysis

Although the first hint for the presence of a pulsation came from *Swift*/XRT data (Rodriguez et al., 2009), we focus here only on the data from *RXTE*/PCA which is the instrument dedicated to the timing analysis of astrophysical sources. Also, we only consider here Obs. X1 and X3 which both have 2 PCUs on and exposure times longer than 2.5 ks, in order to increase the statistical significance of the pulse. We produced power spectral density (PSD) distributions between 0.00195 and 1024 Hz with `powspec v1.0` averaging all sub-intervals of 512 s long of each of the two observations. The continuum of the 0.00195–1024 Hz PSD is equally well represented by a model consisting of a constant (to account for the contribution of Poisson noise), and either a power law (of index $\Gamma = -1.35 \pm 0.08$) or a zero-centred Lorentzian (with a width of $1.6 \pm 0.4 \times 10^{-2}$ Hz). Fig. 4 displays the white-noise corrected PSD restricted to the 0.00195–1 Hz range. Above ~ 0.5 Hz, the PSD is compatible with white noise. A strong peak at around 0.08 Hz and its first harmonic at about 0.16 Hz can be seen above the PSD continuum (Fig. 4). The main peak (at 0.08 Hz) is contained within a single frequency bin which is indicative of a coherent pulsation. However, we point out that the bottom of this thin peak is broadened. This broad feature can be fitted with a Lorentzian of centroid frequency 0.078 ± 0.002 Hz, and a width of 0.020 ± 0.008 Hz. It has a (raw) power of 11.1% RMS. We also note the presence of a possible feature at ~ 0.035 Hz, yet the inclusion of a second Lorentzian to the model does not improve the fit in a significant way. To study the properties of the coherent pulsation, we barycentred the 1-s light curves with `barycorr v1.8` using the orbital ephemeris of the satellite, and we corrected the light curves for the background. The pulsation period was searched for using a Lomb-Scargle periodogram as described in Press & Rybicki (1989) with the errors calculated from the peri-

Table 3. Results of the X-ray spectral fitting. The errors are at the 90% confidence level.

Obs	N_H ($\times 10^{22}$ cm^{-2})	Γ	kT_{bb} (keV)	$F_{2-10,unabs.}$ (erg cm^{-2} s^{-1})	$\chi^{2\star}_{\nu}$ (DOF†)
S1	$4.0^{+0.9}_{-0.8}$	0.9±0.2		3.6×10^{-11}	1.0 (66)
	2.0±0.4		2.1±0.2	3.0×10^{-11}	0.86 (66)
S2	$3.4^{+1.0}_{-0.8}$	1.0±0.3		3.8×10^{-11}	0.78 (34)
	1.8±0.5		$1.8^{+0.3}_{-0.2}$	3.0×10^{-11}	0.74 (34)
X1	3.4 (Frozen)	$1.17^{+0.14}_{-0.11}$		2.65×10^{-11}	0.94 (25)
X2	3.4 (Frozen)	$1.0^{+0.3}_{-0.2}$		0.9×10^{-11}	0.49 (10)
X3	3.4 (Frozen)	1.2±0.1		2.6×10^{-11}	0.91 (25)
X4	3.4 (Frozen)	1.1±0.4		1.1×10^{-11}	0.93 (12)
S3+X5	$3.4^{+1.5}_{-1.6}$	$1.2^{+0.3}_{-0.4}$		0.74×10^{-11}	0.86 (8)

* Reduced χ^2.
† Degrees of freedom.

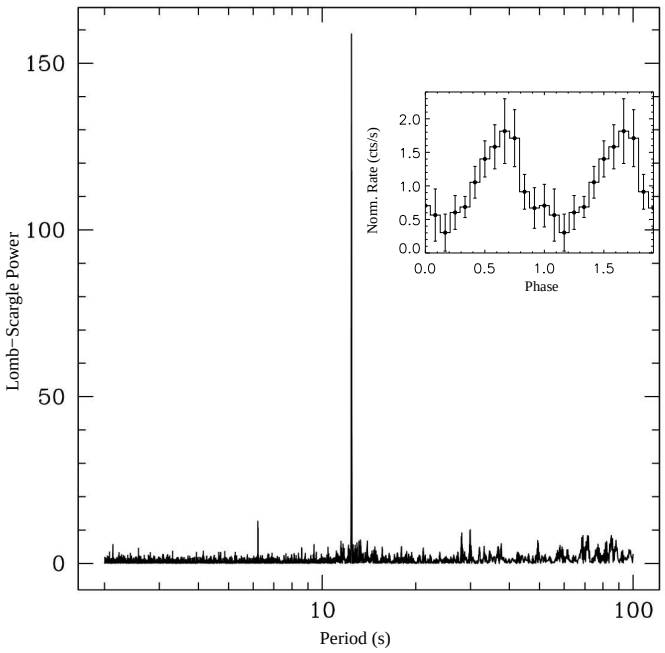

Fig. 5. Lomb-Scargle periodogram of *RXTE* Obs. 1 & 3. The prominent peak is found at a period of ∼ 12.44 s. The insert shows the light curve folded at 12.44 s.

odogram following Horne & Baliunas (1986) (see also the original work of Kovacs, 1981). This is the same method used by Rodriguez et al. (2006) to find the pulse's most precise period in IGR J16320−4751. The light curves were folded with `efold v1.1`. We combined Obs. X1 & X3 to obtain the most precise measure of the pulsation. A very prominent peak is visible in the periodogram (Fig. 5), together with its first harmonic. We derived a pulse period of P=12.43781(3) s (0.080400 Hz). The light curve, folded at a period of 12.44 s, is shown in Fig. 5 as an insert. The pulse fraction was calculated in a standard way ($P = \frac{I_{max}-I_{min}}{I_{max}+I_{min}}$, see e.g. Rodriguez et al., 2006). Without taking the emission of the Galactic ridge into account, we estimate a pulse fraction $P = 28 \pm 2.3\%$. Given the source's location in the Galactic plane which has a non-negligible contribution to the total flux, this value underestimates the true pulse fraction, and should be considered as a lower limit. According to the results of the spectral analysis presented in the previous section, we obtained the "true" background following Eq. 1, which includes the estimated contribution from the Galactic ridge at the position of IGR J19294+1816. The light curves corrected for this total background yields $P = 40 \pm 4.4\%$.

7. Discussion and conclusions

We have reported here the results obtained from a multi-instrumental campaign dedicated to the X-ray properties of new *INTEGRAL* sources. The refinement of the X-ray position provided by the *Swift*/XRT observations enabled us to identify a possible counterpart at infrared wavelengths. The differences of dereddened magnitudes (Table 2) do not lead to any of the spectral types tabulated in Tokunaga (2000). With N_H=2.0×10^{22} cm^{-2}, J−H=0.28 would indicate an F7 V or F8 I star. However the value of H−K_s is inconsistent with both possibilities. With N_H=2.73×10^{22} cm^{-2}, J−H seems too high for any spectral type, although we remark a marginal compatibility (at the edge of the errors on the magnitude) with an O9.5 V star (J−H=−0.13, H−K_s=−0.04 Tokunaga, 2000). This value is, however, a measure of the interstellar absorption through the whole Galaxy. Since IGR J19294+1816 probably lies closer than the other end of the Galaxy, it is likely that the interstellar absorption along the line of sight is lower. In particular, we note that with N_H=2.5×10^{22} cm^{-2}, we obtain J−H=−0.04 and H−K_s=0.05, which is very close to the values tabulated for a B3 I star (J−H=−0.03, H−K_s=0.03 Tokunaga, 2000). In that case, the source would lie at a distance $d \gtrsim 8$ kpc.

The X-ray behaviour of the source is indicative of an HMXB: the X-ray spectra are power law like in shape with a hard photon index. One of the spectra (Obs. S1 with the longest exposure) shows evidence for absorption in clear excess to the absorption on the line of sight, which may indicate some intrinsic absorption in this source. However, the evidence is marginal in the other spectra, which could suggest that the intrinsic absorption varies in this system, as has been observed in a number of HMXBs. A long-term periodicity was revealed in the *Swift*/BAT data which confirms the binarity of the source (Corbet & Krimm, 2009). We clearly detect an X-ray pulse at a period of 12.44 s, indicating the presence of an X-ray pulsar. We estimate a pulse fraction P = 40%. Apart from millisecond X-ray pulsars, found in systems that are at the end of the evolutionary path of X-ray binaries (and are LMXBs), pulsars are young objects that are usually found in HMXBs. We also remark that the PSD of IGR J19294+1816 shows a broadening at the bottom of the coherent pulsation. Sidelobes and other noise features around coherent pulsation signals have been seen in other HMXBs (e.g. Kommers et al.,

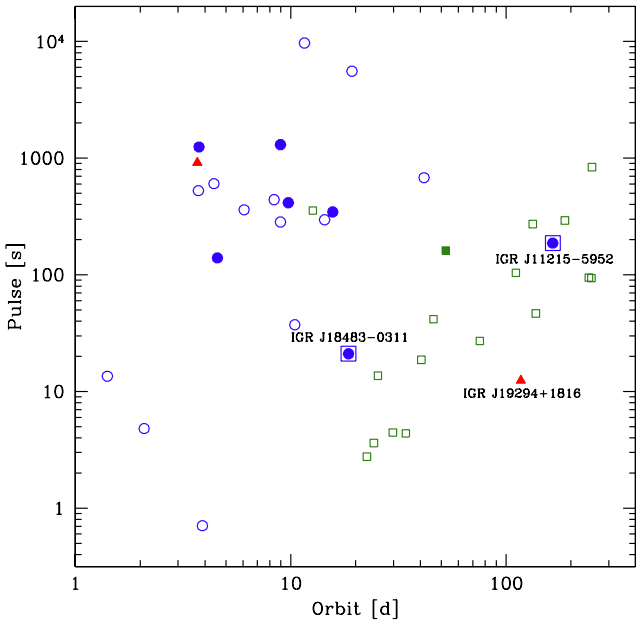

Fig. 6. Most recent version of the "Corbet diagram" including all sources detected with *INTEGRAL* (Bodaghee et al. 2009 in prep.). Squares represent Be-HMXBs, circles Supergiant-HMXBs (Sg-HMXB), circles in squares are SFXTs, filled symbols represent sources discovered by *INTEGRAL*. The triangles are HMXBs of unknown nature (including IGR J19294+1816). The positions of IGR J19294+1816 and of the two SFXTs lying in the Be region of the plot are highlighted.

1998; Kaur et al., 2007, in, respectively, 4U 1626−67, and XTE J0111.2−7317). Such features can be produced by artificial effects (such as the finite length of the time intervals used to make the PSD), or they can be real if, e.g., a quasi-periodic oscillation (QPO) beats with the coherent signal (Kommers et al., 1998; Kaur et al., 2007). In the case of IGR J19294+1816, a possible QPO might be present at ∼ 0.035 Hz (Fig. 4), even if the quality of the data does not allow us to firmly establish its presence. On the other hand, we cannot exclude that the 0.078 Hz feature is itself a QPO at a frequency close to that of the coherent pulsation. Given the faintness of the source, we cannot conclude further on that matter.

In fact, IGR J19294+1816 lies in a region populated by Be-HMXBs in the so-called "Corbet diagram" (Corbet, 1986; Corbet & Krimm, 2009), as demonstrated in Fig. 6. Note that this plot is the most recent update of the Corbet diagram for *INTEGRAL* sources as of June, 2009 (Bodaghee et al. 2009 in prep.). Recently, Bodaghee et al. (2007) further explored the parameter spaces occupied by high-energy sources. They noticed that Be-HMXB and supergiant HMXB also segregate in different parts of the N_H vs. orbital period and N_H vs. spin period diagrams. The value of the absorption we obtained through our spectral analysis, combined with the values of the spin and orbital periods, make IGR J19294+1816 lie in a region populated by Be-HMXBs in these diagrams as well. At first order, one can easily understand the segregation in these three different diagrams as results of the age, type of accretion, and probable type of orbit. Be systems are younger, and hence have eccentric orbits, longer orbital periods, and shorter spin periods, whereas supergiant systems are older, are mostly circularised with shorter orbital periods, and longer spin periods. In these latter systems, in addition, the compact object is embedded in the wind of the companion (the feed matter for accretion) which explains their (usually) higher intrinsic absorption. In this respect, all our results point towards IGR J19294+1816 being a Be-HMXB (the same conclusion, although only based on the Corbet diagram, was presented by Corbet & Krimm, 2009) .

INTEGRAL has unveiled a new (sub-)type of supergiant HMXB, characterised by short (∼hours) and intense flares seen at X-ray energies: the so-called SFXTs. Models of SFXTs involve stochastic accretion of clumps from the (heterogeneous) wind of the supergiant (e.g. in't Zand, 2005; Negueruela et al., 2006), on top of longer, but fainter, periods of activity (e.g. Sidoli et al., 2007). In this respect, the detection of periods of short and intense flares in IGR J19294+1816 with *INTEGRAL* (Fig. 1), a behaviour typical of SFXTs, raises the possibility that this source belongs to this new class. Its position in the Corbet and the N_H vs. spin or orbital period diagrams (Fig. 6) is not a definitive contradiction to this hypothesis, since systematic X-ray studies of SFXTs have shown that, contrary to other HMXBs, they seem to populate any part of the diagrams. In particular, IGR J18483−0311 and IGR J11215−5952, the only two SFXTs for which both orbital and pulse periods are known, lie in the region of Be-systems in these representations (Fig. 6). The former source has a pulse period of 21.05 s, an orbital period of 18.5 d, and has a B0.5 Ia companion (see Rahoui & Chaty, 2008, and references therein). The latter has a pulse period of about 187 s, an orbital period of about 165 d (e.g. Sidoli et al., 2007; Ducci et al., 2009), and is associated with a B supergiant (Negueruela et al., 2005). To reconcile the fact that they are long period systems with a rather low absorption, an eccentric orbit is invoked. IGR J19294+1816 could be the third member of SFXTs (with a known pulse period) having a long and eccentric orbit. In this case, this may point towards the existence of an evolutionary link between Be-HMXBs and eccentric SFXTs (Liu et al. 2009 in prep.). The quality of the data is not good enough to permit us to make any firm conclusions concerning the nature of the system, and only an identification of the optical counterpart's spectral type will resolve this issue.

Acknowledgements. JR acknowledges useful and productive discussions with Farid Rahoui. We thank the referee for the careful reading of this paper and his/her comments that helped us to improve it. We would like to warmly thank the RXTE and Swift PIs and mission planners for having accepted to perform these observations, and the efficient scheduling in simultaneity with one of the INTEGRAL pointings. AP acknowledges the Italian Space Agency financial support via contract I/008/07/0. JAZH acknowledges the Swiss National Science Foundation for financial support. This research has made use of the USNOFS Image and Catalogue Archive operated by the United States Naval Observatory, Flagstaff Station (http://www.nofs.navy.mil/data/fchpix/) This research has made use of the SIMBAD database, operated at CDS, Strasbourg, France. It also makes use of data products from the Two Micron All Sky Survey, which is a joint project of the University of Massachusetts and the Infrared Processing and Analysis Center/California Institute of Technology, funded by the National Aeronautics and Space Administration and the National Science Foundation. The Digitized Sky Surveys were produced at the Space Telescope Science Institute under U.S. Government grant NAG W-2166. The images of these surveys are based on photographic data obtained using the Oschin Schmidt Telescope on Palomar Mountain and the UK Schmidt Telescope. The plates were processed into the present compressed digital form with the permission of these institutions. The Second Palomar Observatory Sky Survey (POSS-II) was made by the California Institute of Technology with funds from the National Science Foundation, the National Geographic Society, the Sloan Foundation, the Samuel Oschin Foundation, and the Eastman Kodak Corporation.

References

Bodaghee, A., Courvoisier, T. J.-L., Rodriguez, J., et al. 2007, A&A, 467, 585
Cardelli, J. A., Clayton, G. C., & Mathis, J. S. 1989, ApJ, 345, 245

Condon, J. J., Cotton, W. D., Greisen, E. W., et al. 1998, AJ, 115, 1693
Corbet, R. H. D. 1986, MNRAS, 220, 1047
Corbet, R. H. D. & Krimm, H. A. 2009, The Astronomer's Telegram, 2008, 1
Dame, T. M., Hartmann, D., & Thaddeus, P. 2001, ApJ, 547, 792
Ducci, L., Sidoli, L., Mereghetti, S., Paizis, A., & Romano, P. 2009, MNRAS, 398, 2152
Horne, J. H. & Baliunas, S. L. 1986, ApJ, 302, 757
in't Zand, J. J. M. 2005, A&A, 441, L1
Kalberla, P. M. W., Burton, W. B., Hartmann, D., et al. 2005, A&A, 440, 775
Kaur, R., Paul, B., Raichur, H., & Sagar, R. 2007, ApJ, 660, 1409
Kommers, J. M., Chakrabarty, D., & Lewin, W. H. G. 1998, ApJ, 497, L33+
Kovacs, G. 1981, Ap&SS, 78, 175
Negueruela, I., Smith, D. M., & Chaty, S. 2005, The Astronomer's Telegram, 470, 1
Negueruela, I., Smith, D. M., Reig, P., Chaty, S., & Torrejón, J. M. 2006, in ESA Special Publication, Vol. 604, The X-ray Universe 2005, ed. A. Wilson, 165–+
Prat, L., Rodriguez, J., Hannikainen, D. C., & Shaw, S. E. 2008, MNRAS, 389, 301
Predehl, P. & Schmitt, J. H. M. M. 1995, A&A, 293, 889
Press, W. H. & Rybicki, G. B. 1989, ApJ, 338, 277
Rahoui, F. & Chaty, S. 2008, A&A, 492, 163
Rahoui, F., Chaty, S., Lagage, P.-O., & Pantin, E. 2008, A&A, 484, 801
Rodriguez, J., Bodaghee, A., Kaaret, P., et al. 2006, MNRAS, 366, 274
Rodriguez, J., Hannikainen, D. C., Shaw, S. E., et al. 2008a, ApJ, 675, 1436
Rodriguez, J., Tomsick, J. A., & Chaty, S. 2008b, A&A, 482, 731
Rodriguez, J., Tuerler, M., Chaty, S., & Tomsick, J. A. 2009, The Astronomer's Telegram, 1998, 1
Sidoli, L., Romano, P., Mereghetti, S., et al. 2007, A&A, 476, 1307
Skrutskie, M. F., Cutri, R. M., Stiening, R., et al. 2006, AJ, 131, 1163
Strohmayer, T., Rodriguez, J., Markwardt, C., et al. 2009, The Astronomer's Telegram, 2002, 1
Tokunaga, A. T. 2000, Infrared Astronomy, ed. A. N. Cox, 143–+
Tuerler, M., Rodriguez, J., & Ferrigno, C. 2009, The Astronomer's Telegram, 1997, 1
Valinia, A. & Marshall, F. E. 1998, ApJ, 505, 134